Fast Fixed-Time Output Multi-Formation Tracking of Networked Autonomous Surface Vehicles: A Mathematical Induction Method

Teng-Fei Ding, *Graduate Student Member, IEEE*, Kun-Ting Xu, Ming-Feng Ge, *Member, IEEE*, Ju H. Park, *Senior Member, IEEE*, and Chang-Duo Liang, *Graduate Student Member, IEEE*

***Abstract*—In this paper, we aim to exploit an effective way to solve the output multi-formation tracking problem of the networked autonomous surface vehicles (ASVs) in a fast fixed time manner. Specifically, addressing the output multi-formation tracking problem implies that 1) the networked ASVs are divided into multiple interconnected subnetworks with respect to multiple targets; 2) for each subnetwork, the outputs of the networked ASVs form a desired geometric formation with exchanging the local interactions. Besides, solving the fast fixed-time tracking problem in this paper implies that 1) the convergence time is independent of the initial conditions; 2) the system states are forced to reach the employed nonsingular fixed-time sliding surface in a prescribed time, which thus called fast fixed-time control. Then, based on a time-related function and a nonsingular fixed-time sliding surface, a hierarchical fast fixed-time control algorithm is proposed to solve the aforementioned problem within a fast fixed time being independent of the initial conditions. Furthermore, by employing the Lyapunov argument and mathematical induction, we present the sufficient conditions for fast fixed-time convergence of the tracking errors with respect to multiple targets. Finally, numerous simulation examples are presented to demonstrate the effectiveness of the proposed control algorithm.**

***Index Terms*—Output multi-formation tracking, hierarchical fast fixed-time control, networked autonomous surface vehicles (ASVs).**

Manuscript received 16 July 2022; revised 14 November 2022; accepted 25 December 2022. Date of publication 4 January 2023; date of current version 18 May 2023. This work of Ju H. Park was supported by the National Research Foundation of Korea (NRF) funded by the Korea Government (Ministry of Science and ICT) under Grant 2019R1A5A8080290. This work was supported in part by the National Natural Science Foundation of China under Grants 62073301 and 52027806, in part by the National Key Technology R&D Program of China under Grants 2020YFB1709301 and 2020YFB1709304, in part by the Natural Science Foundation of Hubei Province of China under Grant 2021CFB516, in part by the Innovative Development Project for Supporting Enterprise Technology of Hubei Province of China under Grant 2021BAB094, and in part by the Open Project of Key Laboratory of Image Processing and Intelligent Control (Huazhong University of Science and Technology), Ministry of Education. The review of this article was coordinated by Dr. Dinh-Thuan Do. *(Corresponding authors: Ming-Feng Ge; Ju H. Park.)*

Teng-Fei Ding is with the School of Mechanical Engineering and Electronic Information, China University of Geosciences, Wuhan 430074, China, and also with Key Laboratory of Image Processing and Intelligent Control, Ministry of Education, Huazhong University of Science and Technology, Wuhan 430074, China (e-mail: dingtf@cug.edu.cn).

Kun-Ting Xu, Ming-Feng Ge, and Chang-Duo Liang are with the School of Mechanical Engineering and Electronic Information, China University of Geosciences, Wuhan 430074, China (e-mail: 1138469431@cug.edu.cn; gemf@cug.edu.cn; liangchangduo93@163.com).

Ju H. Park is with the School of Department of Electrical Engineering, Yeungnam University, Gyeongsan 38541, South Korea (e-mail: jessie@ynu.ac.kr).

Digital Object Identifier 10.1109/TVT.2022.3233887

I. Introduction

AUTONOMOUS surface vehicles (ASVs) are a class of intelligent surface vessels with self-navigation capability, and have been widely applied to accomplish different practical tasks, including water quality measurement, target detection, military reconnaissance and other tasks [1], [2], [3]. Compared with a single ASV, the networked ASVs admits information exchange, cooperation, task assignments, design of decentralized algorithms among different individuals, thus possessing the characteristics of higher working efficiency, higher fault-tolerant capability, stronger robustness and more flexibility [4]. This then motivats people to develop different control strategies for networked ASVs to achieve different control goals, including containment control [5], [6], formation control [7], [8], trajectory tracking [9], [10], [11], path following [12], [13] and target tracking [11], [14]. Among the above-mentioned collective goals of the networked ASVs, formation control has been recognized as one of the most fundamental objectives, aiming to drive the networked ASVs to form a desired formation configuration for some user-assigned missions.

The formation control has been researched extensively owing to its wide applications. On the one hand, from the perspective of control objectives, formation control can be classified into single-formation and multi-formation, where the controlled systems are requested to perform single or multiple missions respectively. The existing researches are mainly concentrate on single-formation control, which aims to urge multiple ASVs into a single formation pattern [15], [16], [17], [18]. Besides, in the multi-formation control [19], [20], [21], the overall interaction networks are generally segmented into several subnetworks and each subnetwork form a formation pattern respectively. On the other hand, from the perspective of control theory, formation control can be categorized into state formation and output formation, where the formation maneuvering is utilized by state coordination or output coordination. Different from the state formation control studied in [22], [23], the problem of output formation is more significance from the aspect of engineering

application [24], [25]. Despite the rich literature in the area of formation control, there are less references on the combination of multi-formation control and output formation control (i.e., output multi-formation control) for the networked ASVs due to its highly complicated nonlinear controlled system and the complex interaction behaviors.

In addition, the convergence speed is also a significant concern in the coordinated control area owing to its vital index in assessing the quality of the designed control protocols. The finite-time control [26], [27], [28] generally performs faster convergence rate than asymptotic convergence [29], [30], [31]. However, the settling time of the finite-time control is related to the initial conditions, which weakens its practicability in some scenarios. To loosen this restriction, the fixed-time control has been proposed in [11], [32], [33], in which the settling time can be prescribed arbitrarily by adjusting several constrained parameters. Recently, some user-assignable time control methods have already arisen to alleviate the uncertainty of the settling time. The relevant references can be mainly classified into prescribed-time stability [34], [35] and predefined-time stability [36], [37], [38], in which the settling time can be viewed as a parameter in the designed algorithm and thus allowed to be user-assigned arbitrarily. Motivated by the existing fixed-time control and prescribed-time control, we aim to exploit a new control algorithm to combine the both two control technologies for achieving a newly designed fast fixed-time control by simultaneously considering the issues of output multi-formation, uncertainty and nonlinear models.

Consequently, inspired by the above discussions, we propose a novel fast fixed-time control algorithm for the networked ASVs with uncertain disturbances and devote to achieve the output multi-formation tracking in the fast fixed time. The designed control algorithm includes the distributed prescribed-time estimator layer and the local control layer. Based on a time-related function, the states of the leader are estimated in a prescribed time at the distributed estimator layer. Then, based on a nonsingular fixed-time sliding surface and the same time-related function, the controlled system is forced to reach the sliding surface in a prescribed time. This can be further derived that the output multi-formation tracking problem is solved in a fast fixed time. Further, both the Lyapunov stability theory and mathematical induction method are employed to obtain the sufficient conditions. The main highlights are summarized as follows.

1) Different from the finite-time control algorithms [26], [27], [28], where the convergence time is related to the initial conditions. The proposed fast fixed-time control algorithm reduces this constraint. Different from the fixed-time sliding mode control [39], in which the reaching time is relevant to the multiple control gains and can not be determined easily. The reaching time of the proposed algorithm can be prescribed arbitrary by choosing a parameter, even to an extremely small value.
2) Different from the researches on multi-target tracking problem in asymptotic convergence [19] and finite-time convergence [20], [21], we solve the fast fixed-time output multi-formation tracking problem of the networked ASVs successfully for the first time.

TABLE I
NOTATIONS OF SYMBOLS

Notations	Representative
I_n	the n order identity matrix
$\otimes$	the Kronecker product
$\tanh(\cdot)$	the normal standard $\tanh$ function
$\mathrm{sgn}(\cdot)$	the normal standard sign function
$\|\cdot\|$, $\|\cdot\|_1$	the 2-norm and the 1-norm
$\|\cdot\|$	the absolute value
$\mathbf{1}(\mathbf{0})$	the vector where all the elements are $1(0)$

3) Different from the conventional analytical method of the dynamic stability [34], [35], we provide a method combining mathematical induction and Lyapunov function to analyze the prescribed stability of the controlled system.

The remainder of this paper is organized as follows. The preliminaries and problem formulation are given in Section II. The main results are given in Section III, in which the designed algorithm is presented and analyzed completely. The simulation results are presented and discussed in Section VI. Finally, conclusions are summarized in Section V.

II. Preliminaries and Problem Formulation

A. Graph Theory

A directed graph $\mathcal{G} = \{\mathcal{V}, \mathcal{E}, \mathcal{A}\}$ is introduced to indicate the interaction of the networked ASVs, where $\mathcal{V} = \{1, 2, \ldots, N\}$, $\mathcal{E} \in \mathcal{V} \times \mathcal{V}$, and $\mathcal{A} = [\wp_{ij}] \in \mathbb{R}^{N\times N}$. $(i, j) \in \mathcal{E}$ indicates that $\wp_{ij} > 0$, $\wp_{ij} = 0$ otherwise. The neighbor set of the ith ASV is defined as $\mathcal{N}_i = \{j \in \mathcal{V} | (i, j) \in \mathcal{E}\}$. The Laplacian matrix $\mathcal{L} = [l_{ij}] \in \mathbb{R}^{N\times N}$ with $l_{ii} = \sum_{j=1}^{N} \wp_{ij}, i = j \in \mathcal{V}$ and $l_{ij} = -\wp_{ij}$, $i \neq j \in \mathcal{V}$. Spontaneously, $\mathcal{B} = \mathrm{diag}(\wp_{10}, \ldots, \wp_{N0})$ is defined to depict the interaction between the ith ASV and its corresponding tracking target. $\wp_{i0} > 0$ if the ith ASV can receive information from the target directly, otherwise $\wp_{i0} = 0$.

For the interaction of the networked ASVs in multi-formation tracking control, consider that the networked ASVs are divided into $J (1 \leq J \leq N)$ groups, each of which has the same tracking target and the related interaction can be depicted by subgraph $\mathcal{G}_l = \{\mathcal{V}_l, \mathcal{E}_l, \mathcal{A}_l\}$, $l \in \{1, \ldots, J\}$, the corresponding node sets are divided into $\{\mathcal{V}_1, \mathcal{V}_2, \ldots \mathcal{V}_J\}$. Particularly, $\mathcal{V}_l \cap \mathcal{V}_m = \emptyset$, $\forall l \neq m$ and $l, m \in \{1, \ldots, J\}$. Employing n_l labeled the number of ASVs in each group, one has $\sum_{l=1}^{J} n_l = N$ and $\mathcal{V}_l = \{1 + \sum_{i=1}^{l} n_{i-1}, \ldots, \sum_{i=1}^{l} n_i\}$. Similarly, $\mathcal{B}_l$ is the pinning matrix of subgraph $\mathcal{G}_l$.

Assumption 1: For each subgraph $\mathcal{G}_l$, $l \in \{1, 2, \ldots, J\}$, the information of the sub-leaders is globally accessible to all its follower vehicles.

Assumption 2: The directed graph $\mathcal{G}$ with acyclic partition satisfy the in-degree balanced condition, i.e., each row sum of $\mathcal{L}_{lm}$ is zero.

According to [40, Lemma 1], the Laplacian matrix can be rewritten into the following form for the directed graph $\mathcal{G}$ with

acyclic partition.

$$\mathcal{L}=\begin{bmatrix}\mathcal{L}_1 & 0 & \dots & 0\\ \mathcal{L}_{21} & \mathcal{L}_2 & \dots & 0\\ \vdots & \vdots & \ddots & \vdots\\ \mathcal{L}_{J1} & \mathcal{L}_{J2} & \dots & \mathcal{L}_J\end{bmatrix},$$

where $\mathcal{L}_l$ is the laplacian matrix of $\mathcal{G}_l$, $\mathcal{L}_{lm}$ denotes the interaction between subgroup $\mathcal{G}_l$ and $\mathcal{G}_m$, $\forall l\neq m, l, m\in\{1,\dots,J\}$.

B. Definitions and Lemmas

Definition 1: The system $\dot{x}=f(x,t)$, $x(0)=x_0$, is said to be fixed-time stable if there exists a positive constant $T_{\max}>0$ such that $f(x(t))=0, \forall t\geq T_{\max}$, where $T_{\max}>T(x_0), T(x_0)$ is globally finite-time stable with settling-time function.

Definition 2: The system $\dot{x}=f(x,t)$ is said to be prescribed-time stable if there are two constants δ and T such that $\|x(t)\|\leq\delta$ for any initial conditions when $t\geq T$, where T can be prescribed freely.

Lemma 1: [35] Consider that there exists a continuous differentiable Lyapunov function $V(y)$ such that $\dot{V}(y)\leq -bV(y)-c\varphi(t)V(y)$, where $b\geq 0, c>0$, and $\varphi(t)$ is presented as

$$\varphi(t)=\begin{cases}\frac{\dot{\mu}(t)}{\mu(t)}, t_0\leq t<t_0+T_u,\\ \frac{\rho}{T_u}, t\geq t_0+T_u,\end{cases}\tag{1}$$

where the time-related function $\mu(t)$ is proposed as

$$\mu(t)=\left(\frac{T_u}{t_0+T_u-t}\right)^{\rho}, t\in[t_0,t_0+T_u),\tag{2}$$

in which $\rho>1$ is a real number, $t_0>0$ and $T_u>0$ are the initial time and the user-prescribed time. Beside, it holds that $V(y)\leq \mu^{-c}(t)\exp^{-b(t-t_0)}V(t_0)$ on $t\in[t_0,t_0+T_u)$ and $V(y)=0$ on $t\in[t_0+T_u,\infty)$.

Lemma 2: [41] Under Assumption 1, for each subgraph $\mathcal{G}_l$, $l\in\{1,2,\dots,J\}$, there exist two positive-defined matrices P and Q such that

$$Q=PH+H^TP,\tag{3}$$

where $H=\mathcal{L}+\mathcal{B}$ is a nonsingular matrix, $x=[x_1,x_2,\dots,x_N]^T=H^{-1}\mathbf{1}_N$, $y=[y_1,y_2,\dots y_N]^T=H^{-T}\mathbf{1}_N$, $P=\mathrm{diag}(\zeta_i)=\mathrm{diag}(y_i/x_i)$.

Lemma 3: [42] For each subgraph $\mathcal{G}_l, l\in\{1,2,\dots,J\}$, there is a positive-defined matrix $\Xi=\mathrm{diag}(\epsilon_1,\epsilon_2,\dots,\epsilon_N)$ such that

$$\varpi^T\Xi L\mathrm{sgn}(\varpi)\geq 0,\ \forall\varpi=(\varpi_1,\varpi_2,\dots,\varpi_N)^T\in\mathbb{R}^N.\tag{4}$$

Lemma 4: [43]There exists a positive constant $\hbar$ such that

$$\|x\|\,\|y\|\leq\hbar\|x\|^2+\frac{1}{4\hbar}\|y\|^2.\tag{5}$$

where x, y are vectors arbitrarily.

C. System Formulation

Consider that the networked ASVs include N individuals. The dynamics and kinematics of the ith ASV with port-starboard symmetric model are established as follows [44].

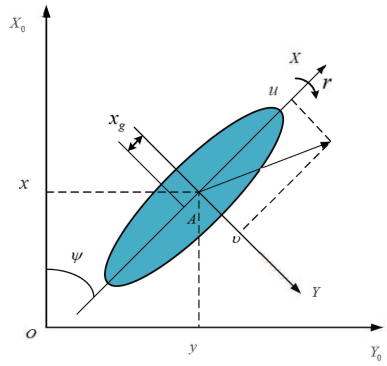

Fig. 1. The reference coordinate frame of a single ASV.

$$\begin{cases}\dot{\eta}_i=R(\psi_i)v_i,\\ M_i\dot{v}_i+C_i(v_i)v_i+D_i(v_i)v_i=\tau_i+d_i(t),\end{cases}\tag{6}$$

where $\eta_i=[x_i,y_i,\psi_i]^T\in\mathbb{R}^3$ and $v_i=[u_i,\upsilon_i,r_i]^T\in\mathbb{R}^3$ are ASVs' states. $[x_i,y_i]^T\in\mathbb{R}^2$ is the position and ψ_i is the heading angle in the earth-fixed frame (OX_0Y_0). $[u_i,\upsilon_i]^T\in\mathbb{R}^2$ is the velocity and r_i is the angular rate in the body-fixed frame (AXY). More details refer to Fig. 1. $\tau_i=[\tau_{i1},\tau_{i2},\tau_{i3}]^T\in\mathbb{R}^3$ is the control input. $d_i(t)=[d_{i1}(t),d_{i2}(t),d_{i3}(t)]^T\in\mathbb{R}^3$ is the bounded external disturbances. The positive-definite and symmetric inertia parameter matrix M_i, the Coriolis and centripetal terms $C_i(v_i)$ and damping matrix $D_i(v_i)$ are the dynamical terms of the vehicle, whose specific mathematical formulation are proposed in Appendix C. Besides, the rotation matrix $R(\psi_i)$ is defined as

$$R(\psi_i)=\begin{bmatrix}\cos(\psi_i) & -\sin(\psi_i) & 0\\ \sin(\psi_i) & \cos(\psi_i) & 0\\ 0 & 0 & 1\end{bmatrix},$$

with the following relevant properties

$$\begin{aligned}&R^T(\psi_i)R(\psi_i)=I,\\ &\|R(\psi_i)\|=1,\\ &\dot{R}(\psi_i)=R(\psi_i)S(r_i),\end{aligned}\tag{7}$$

where $S(r_i)=\begin{bmatrix}0 & -r_i & 0\\ r_i & 0 & 0\\ 0 & 0 & 0\end{bmatrix}$. Additionally, define the velocity of the networked ASVs in the earth-fixed frame as

$$w_i=R(\psi_i)v_i,\tag{8}$$

where $w_i=[w_{i1},w_{i2},w_{i3}]^T\in\mathbb{R}^3$. Combing with the properties (7), (6) can be redefined as

$$\begin{cases}\dot{\eta}_i=w_i,\\ \dot{w}_i=A_i(\eta_i)\tau_i+Y_i(\eta_i,v_i)+\bar{d}_i(t),\end{cases}\tag{9}$$

where $A_i(\eta_i)=R(\psi_i)M_i^{-1}$, $Y_i(\eta_i,v_i)=R(\psi_i)S(r_i)v_i-A_i(\eta_i)(D_i(v_i)+C_i(v_i))v_i$, $\bar{d}_i(t)=A_i(\eta_i)d_i(t)$.

The leaders in multi-formation tracking control are modeled as $\dot{\eta}_l^0=w_l^0$ and $\dot{w}_l^0=a_l^0$, $\forall l\in\{1,2,\dots,J\}$, where ${\eta_l}^0$, ${w_l}^0$,

${a_l}^0$ are the position, velocity and acceleration in the earth-fixed frame.

Assumption 3: The derivatives of all the leaders' accelerations are bounded, namely, $\|\dot{a}_l^0\| \leq d_a$, $\forall l \in \{1, 2, \ldots, J\}$, where $d_a > 0$.

Assumption 4: The external disturbances are bounded, namely, $\|\bar{d}_i(t)\| \leq d_m$, where $d_m > 0$.

D. Control Objective

Definition 3: For the system (6), the fast fixed-time output multi-formation tracking control problem could be solved if there exists a fixed time $T > 0$ such that

$$\begin{cases} \lim\limits_{t\to T} \left\|\eta_i - \eta_l^0 - o_i\right\| = 0, \\ \lim\limits_{t\to T} \left\|w_i - w_l^0\right\| = 0, \end{cases} \tag{10}$$

as well as $\|\eta_i - \eta_l^0 - o_i\| \equiv 0$ and $\|w_i - w_l^0\| \equiv 0$ for all $t \in [T, \infty)$, $\forall i \in \mathcal{V}$, $l \in \{1, 2, \ldots, J\}$, where o_i is the formation offset.

III. Main Results

A. The Fast Fixed-Time Tracking Algorithm

The hierarchical fast fixed-time tracking algorithm is designed to solve the output multi-formation tracking problem in the fast fixed time. To this end, a distributed prescribed-time estimator is designed to estimate the leaders' states, and then a nonsingular fixed-time sliding surface is introduced to constitute the local control layer, as well as a time-related function applied to force the system states reaching the sliding surface in the prescribed time. For the distributed prescribed-time estimator, the algorithm is designed as

$$\begin{cases} \dot{\hat{\eta}}_i = \hat{w}_i, \\ \dot{\hat{w}}_i = -\alpha_1 \varphi^2(t) \left(\sum\limits_{j\in\mathcal{N}_i} \wp_{ij}(\hat{\eta}_i - \hat{\eta}_j) + \wp_{i0}(\hat{\eta}_i - \eta_l^0) \right) \\ \quad + \hat{a}_i - \alpha_2 \varphi(t) \left(\sum\limits_{j\in\mathcal{N}_i} \wp_{ij}(\hat{w}_i - \hat{w}_j) + \wp_{i0}(\hat{w}_i - w_l^0) \right), \\ \dot{\hat{a}}_i = -\alpha_3 \left(\beta_1 + \beta_2 \varphi(t)\right) \left(\sum\limits_{j\in\mathcal{N}_i} \wp_{ij}(\hat{a}_i - \hat{a}_j) \right. \\ \quad \left. + \wp_{i0}(\hat{a}_i - a_l^0) \right) \\ \quad -\beta_3 \mathrm{sgn} \left(\sum\limits_{j\in\mathcal{N}_i} \wp_{ij}(\hat{a}_i - \hat{a}_j) + \wp_{i0}(\hat{a}_i - a_l^0) \right), \end{cases} \tag{11}$$

where $\hat{\eta}_i$, $\hat{w}_i$ and $\hat{a}_i$ are the estimator of η_l^0, w_l^0 and a_l^0 in the earth-fixed frame, $\alpha_1, \alpha_2, \alpha_3, \beta_1, \beta_2, \beta_3 \geq d_a$ are positive parameters, $\varphi(t)$ has been defined in (1). Before move on, define the tracking errors as

$$e_i = \eta_i - \hat{\eta}_i - o_i, \dot{e}_i = \dot{\eta}_i - \hat{w}_i, \tag{12}$$

where o_i is the formation offset. Then for the local control layer, the algorithm is designed as

$$\begin{cases} \tau_i = \tau_{i0} + \tau_{i1} + \tau_{i2}, \\ \tau_{i0} = -A_i^{-1}(\eta_i) \left({\gamma_2}^{-1} \left|\dot{e}_i\right|^{1-\gamma_2} \left(\tilde{K}\left(e_i\right) \dot{e}_i + K_i\left(e_i\right) \dot{e}_i \right) \right. \\ \quad \left. -\hat{a}_i + Y_i(\eta_i, v_i) \right), \\ \tau_{i1} = -{\gamma_2}^{-1} \delta_\xi \left(\left|\dot{e}_i\right|^{\gamma_2 - 1} \right) A_i^{-1}(\eta_i) \left|\dot{e}_i\right|^{1-\gamma_2} \\ \quad \times (\gamma_3 + 2\gamma_4 \varphi(t)) s_i, \\ \tau_{i2} = -A_i^{-1}(\eta_i) \Pi_i \tanh\left(s_i\right), \end{cases} \tag{13}$$

where

$$s_i = K_i\left(e_i\right) e_i + \mathrm{sig}^{\gamma_2}\left(\dot{e}_i\right), \tag{14}$$

$$K_i\left(e_i\right) = \left(k_1 |e_i|^{\gamma - \frac{1}{k\gamma_2}} + k_2 |e_i|^{\gamma_1 - \frac{1}{k\gamma_2}} \right)^{k\gamma_2},$$

$$\begin{aligned} \tilde{K}\left(e_i\right) = k\gamma_2 & \left(k_1 |e_i|^{\gamma - \frac{1}{k\gamma_2}} + k_2 |e_i|^{\gamma_1 - \frac{1}{k\gamma_2}} \right)^{k\gamma_2 - 1} \\ & \times \left(k_1 \left(\gamma - \frac{1}{k\gamma_2} \right) |e_i|^{\gamma - \frac{1}{k\gamma_2}} \right. \\ & \left. + k_2 \left(\gamma_1 - \frac{1}{k\gamma_2} \right) |e_i|^{\gamma_1 - \frac{1}{k\gamma_2}} \right), \end{aligned}$$

$$\delta_\xi(x) = \begin{cases} \sin\left(\frac{\pi}{2} \frac{x^2}{\xi^2} \right), |x| \leq \xi, \\ 1, |x| > \xi, \end{cases}$$

$\mathrm{sig}(x)^\gamma = \mathrm{col}(\mathrm{sgn}(x_1)|x_1|^\gamma, \mathrm{sgn}(x_2)|x_2|^\gamma, \ldots, \mathrm{sgn}(x_n)|x_n|^\gamma)$, $k, k_1, k_2, \gamma, \gamma_1, \gamma_2$ are subject to $\gamma_1 k > 1, 1 < \gamma_2 \leq 2, k > 1, 1/\gamma_2 < \gamma k < 1$, ξ is a designed parameter, $\delta_\xi(x)$ is non-negative with the property of $\delta_\xi(x)/x \to 0$ when $x \to 0$, which guarantees the control input is well-defined even when tracking errors converge to orgin. Π_i is a diagonal matrix with positive designed gains. According to [39, Lemma 4], once the nonsingular sliding surface $s_i = 0$ is satisfied, e_i and $\dot{e}_i$ converge to the origin in the fixed time T_κ, which is bounded with

$$T_\kappa \leq \frac{1}{{\alpha_1}^k (1 - \gamma k)} + \frac{1}{{\alpha_2}^k (\gamma_1 k - 1)}. \tag{15}$$

Remark 1: Noting that the implement of sliding mode control (SMC) generally contains two-stage process. Firstly, the controlled system is drived to reach the sliding surface. Secondly, the system states remains on the sliding surface and then reach to the origin within infinite time. Compared with the conversional SMC, the control strategy in this paper has the following advantages. 1) the controlled systems are drived to reach the sliding surface in the prescribed time, which can be predesigned arbitrary; 2) the system states reach to the origin within fixed time without the existence of the singularity problem. Superiorly, compared with the conversional fixed-time sliding mode control, the designed algorithm has a faster settling time due to the existence of the time-related function in some sense.

Remark 2: Compared with the existing fixed-time algorithms, the designed fast fixed-time controller shows faster convergence gate in the following aspects.

1) In [15], [45], the fixed-time observers are employed to estimate the leaders states in a fixed time, where the settling time is a bounded constant that related to multiple control gains and thus can not be prescribed easily. The designed estimator (11) can estimate the states of the leader in the prescribed time, which can be predetermined arbitrarily to an extremely small value by selecting only one parameter. This is one reason for achieving the fast convergence rate.
2) Compared with [15], [46], where the settling time of reaching the fixed-time sliding surface is always in connection with several control parameters. The prescribed-time reachability of the designed algorithm is guaranteed by selecting an arbitrary small constant. This is another reason for achieving the fast convergence rate.
3) Different from [18], [47], where the fast convergence rate is achieved by using the fixed-time sliding mode control approach. We present a novel framework for achieving the fast fixed-time stability by combining the prescribed-time control with the fixed-time sliding mode control for accelerating the reaching time to the sliding surface.

B. Analysis of the Distributed Prescribed-Time Estimator

Theorem 1: Suppose that Assumptions 1-3 hold. By using (11), the states of the leaders can be estimated in the prescribed-time manner and the prescribed time T_1 can be set as $T_1 = t_o + \sum_{l=1}^{2J} T_u, \forall l \in \{1, 2 \ldots, J\}$, $t_0 > 0$ and $T_u > 0$ are the initial time and the user-prescribed time. Besides, the necessary conditions for the designed control gains are presented as:

$$\begin{aligned} &2 + \alpha_1\rho - \alpha_2 + bT_u + c\rho - \alpha_2\rho\frac{\lambda_{\max}(Q_l)}{\lambda_{\max}(P_l)} \le 0,\\ &\rho\alpha_1 - \alpha_2 \le 0,\\ &\alpha_3 \ge \frac{\lambda_{\max}(P_l)}{\lambda_{\min}(Q_l)},\\ &\beta_3 \ge d_a. \end{aligned} \tag{16}$$

Proof: The proof includes two main steps. In the first step, it will be proved that the third equation of (11) can estimate the acceleration a_l^0 of the leaders in the prescribed time $t_0 + \sum_{l=1}^{J} T_u$, i.e., $\lim_{t\to t_0+\sum_{l=1}^{J} T_u}(\hat{a}_i - a_l^0) = 0$, $\forall i \in \mathcal{V}$, $l \in \{1, 2, \ldots, J\}$. Let $\hat{a} = (\hat{a}_1, \hat{a}_2, \ldots, \hat{a}_N)^T$, $\tilde{e} = H(\hat{a} - a_l^0\mathbf{1})$, where

$$H = \mathcal{L} + \mathcal{B} = \begin{bmatrix} h_{11} & 0 & \ldots & 0 \\ h_{21} & h_{22} & \ldots & 0 \\ \vdots & \vdots & \ddots & 0 \\ h_{J1} & h_{J2} & \ldots & h_{JJ} \end{bmatrix}, \tag{17}$$

in which $h_{ll} = \mathcal{L}_l + \mathcal{B}_l, l \in \{1, 2, \ldots, J\}$. Taking the derivative of $\tilde{e}$ along the acceleration estimator (i.e., the third equation of (11)), and then combing with the specific form of H, we can obtain the expansion of $\dot{\tilde{e}}$ as the following form

$$\begin{aligned} \dot{\tilde{e}}_1 =& -\alpha_3\left(\beta_1 + \beta_2\varphi(t)\right)h_{11}\tilde{e}_1 - \beta_3 h_{11}\mathrm{sgn}(\tilde{e}_1) - \dot{a}_1^0 h_{11}\mathbf{1},\\ \dot{\tilde{e}}_2 =& -\alpha_3\left(\beta_1 + \beta_2\varphi(t)\right)h_{22}\tilde{e}_2 - \beta_3 h_{21}\mathrm{sgn}(\tilde{e}_2) - \dot{a}_2^0 h_{22}\mathbf{1}\\ &-\alpha_3\left(\beta_1 + \beta_2\varphi(t)\right)h_{21}\tilde{e}_1 - \alpha_5 h_{21}\mathrm{sgn}(\tilde{e}_1),\\ &\vdots\\ \dot{\tilde{e}}_J =& -\alpha_3\left(\beta_1 + \beta_2\varphi(t)\right)h_{JJ}\tilde{e}_J - \beta_3 h_{JJ}\mathrm{sgn}(\tilde{e}_J)\\ &-\dot{a}_J^0 h_{JJ}\mathbf{1} - \alpha_3\left(\beta_1 + \beta_2\varphi(t)\right)\sum_{l=1}^{J-1} h_{Jl}\tilde{e}_l\\ &-\beta_3\sum_{l=1}^{J-1} h_{Jl}\mathrm{sgn}(\tilde{e}_l). \end{aligned} \tag{18}$$

The Lyapunov function candidate is expressed as

$$V_{1l} = \frac{1}{2}\tilde{e}_l^T P_l \tilde{e}_l, l \in \{1, 2, \ldots, J\}. \tag{19}$$

The remaining proof is based on the mathematical induction.

Step 1: Suppose $l = 1$. It follows that

$$V_{11} = \frac{1}{2}\tilde{e}_1^T P_1 \tilde{e}_1. \tag{20}$$

For the time interval $[t_0, t_0 + T_u)$, taking the derivative of V_{11}, it can be obtained that

$$\begin{aligned} \dot{V}_{11} = \tilde{e}_1^T P_1[&(-\alpha_3\left(\beta_1 + \beta_2\varphi(t)\right)h_{11}\tilde{e}_1\\ &-\beta_3 h_{11}\mathrm{sgn}(\tilde{e}_1) - \dot{a}_1^0 h_{11}\mathbf{1}]. \end{aligned} \tag{21}$$

Based on Lemma 2 and Lemma 3, the following inequalities hold

$$\begin{aligned} -\tilde{e}_1^T P_1 h_{11}\tilde{e}_1 &= -\frac{1}{2}\tilde{e}_1^T Q_1 \tilde{e}_1,\\ -\tilde{e}_1^T P_1 h_{11}\mathrm{sgn}(\tilde{e}_1) &= -\tilde{e}_1^T(P_1\mathcal{L}_1 + P_1\mathcal{B}_1)\mathrm{sgn}(\tilde{e}_1)\\ &= -\tilde{e}_1^T P_1\mathcal{B}_1\mathrm{sgn}(\tilde{e}_1)\\ &\le \sum_{i=1}^{N}\wp_{i0}p_i\|\tilde{e}_1\|_1,\\ -\tilde{e}_1^T P_1\dot{a}_1^0 h_{11}\mathbf{1} &= -\tilde{e}_1^T P_1\dot{a}_0(\mathcal{L}_1 + \mathcal{B}_1)\mathbf{1}\\ &= -\tilde{e}_1^T P_1\dot{a}_1^0\mathcal{B}_1\mathbf{1}\\ &\le \sum_{i=1}^{N} p_i\wp_{i0}d_a\|\tilde{e}_1\|_1. \end{aligned} \tag{22}$$

where p_i is the ith element of P_1. It then follows that

$$\begin{aligned} \dot{V}_{11} \le& -\frac{1}{2}\alpha_3\left(\beta_1 + \beta_2\varphi(t)\right)\lambda_{\min}(Q_1)\tilde{e}_1^T\tilde{e}_1\\ &-\sum_{i=1}^{N} p_i\wp_{i0}(\beta_3 - d_a)\|\tilde{e}_1\|_1\\ \le& -\frac{1}{2}\alpha_3\left(\beta_1 + \beta_2\varphi(t)\right)\lambda_{\min}(Q_1)\tilde{e}_1^T\tilde{e}_1. \end{aligned} \tag{23}$$

Noting the fact that

$$-\frac{1}{2}\lambda_{\max}(P_1)\tilde{e}_1^T\tilde{e}_1 \le -V_{11} \le -\frac{1}{2}\lambda_{\min}(P_1)\tilde{e}_1^T\tilde{e}_1. \tag{24}$$

It further obtains

$$-\frac{1}{2}\tilde{e}_1^T\tilde{e}_1 \leq -\frac{V_{11}}{\lambda_{\max}(P_1)}. \tag{25}$$

Combing (23) with (25), it derives that

$$\dot{V}_{11} \leq -\alpha_3\left(\beta_1+\beta_2\varphi(t)\right)\frac{\lambda_{\min}(Q_1)}{\lambda_{\max}(P_1)}V_{11}. \tag{26}$$

If (16) holds, it follows that

$$\dot{V}_{11} \leq -\left(\beta_1+\beta_2\varphi(t)\right)V_{11}. \tag{27}$$

It thus can be concluded that $\lim_{t\to t_0+T_u}\|\tilde{e}_1\|=0$. Noting that H is a nonsingular matrix, it thus comes to the conclusion that $\lim_{t\to t_0+T_u}\|\hat{a}_i-a_1^0\|=0$, $\forall i\in\mathcal{V}_1$. For the time interval $[t_0+T_u,+\infty)$, with the similar analysis of (20)-(27), we can derived that $\dot{V}_{11}\leq-(\beta_1+\beta_2\varphi(t))V_{11}$. Then we can derive that $V_{11}=0$ for $t\in[t_0+T_u,+\infty)$.

Step 2: Suppose $l=2$. When $t\geq t_0+T_u$, $\dot{\tilde{e}}_2$ can be redefined as follows

$$\dot{\tilde{e}}_2 = -\alpha_3\left(\beta_1+\beta_2\varphi(t)\right)h_{22}\tilde{e}_2-\beta_3h_{22}\mathrm{sgn}(\tilde{e}_2)-\dot{a}_2^0h_{22}\mathbf{1}. \tag{28}$$

Since $\|\tilde{e}_1\|=0$ for $t\geq t_0+T_u$. Similar to the steps (20)-(27), it can be concluded that $\tilde{e}_2$ converge to the origin as $t\to t_0+2T_u$.

Step 3: For $l=J$, when $t\geq t_0+\sum_{l=1}^{J-1}T_u$, it follows that

$$\begin{aligned}\dot{\tilde{e}}_J = &-\alpha_3\left(\beta_1+\beta_2\varphi(t)\right)h_{JJ}\tilde{e}_J-\beta_3h_{JJ}\mathrm{sgn}(\tilde{e}_J)\\&-\dot{a}_J^0h_{JJ}\mathbf{1}.\end{aligned} \tag{29}$$

Based on the mathematical induction, it can be obtained that all the followers estimate the accelerations of the related sub-leader within the prescribed time $T_{11}=t_0+\sum_{l=1}^{J}T_u$.

In the second step, It will be proved that $\lim_{t_0+\sum_{l=1}^{2J}T_u}\|\hat{\eta}_i-\eta_l^0\|=0$ and $\lim_{t_0+\sum_{l=1}^{2J}T_u}\|\hat{w}_i-w_l^0\|=0$, $\forall i\in\mathcal{V}$, $l\in\{1,2,\ldots,J\}$. Before moving on, let the estimated errors be $\tilde{\eta}_i=\hat{\eta}_i-\eta_l^0$, $\tilde{w}_i=\hat{w}_i-w_l^0$, and the corresponding compact form be $\tilde{\eta}=\mathrm{col}(\tilde{\eta}_1,\tilde{\eta}_2,\ldots,\tilde{\eta}_N)$, $\tilde{w}=\mathrm{col}(\tilde{w}_1,\tilde{w}_2,\ldots,\tilde{w}_N)$. For further analysis, two auxiliary parameters are defined as

$$\begin{aligned}\bar{\eta}_i&=(H\otimes I_3)\varphi(t)\tilde{\eta}_i,\\ \bar{w}_i&=(H\otimes I_3)\tilde{w}_i.\end{aligned} \tag{30}$$

Taking the derivative of $\bar{\eta}_i$ yields that

$$\begin{aligned}\dot{\bar{\eta}}_i&=(H\otimes I_3)[\dot{\varphi}(t)\tilde{\eta}_i+\varphi(t)\tilde{w}_i]\\&=(H\otimes I_3)[\bar{\varphi}(t)\bar{\eta}_i+\varphi(t)\bar{w}_i],\end{aligned} \tag{31}$$

where

$$\bar{\varphi}(t)=\frac{\dot{\varphi}(t)}{\varphi(t)}=\begin{cases}\frac{\varphi(t)}{\rho}, t_0\leq t<t_0+T_u,\\ 0, t\geq t_0+T_u.\end{cases} \tag{32}$$

Let $\bar{\eta}=\mathrm{col}(\bar{\eta}_1,\bar{\eta}_2,\ldots,\bar{\eta}_N)$, $\bar{w}=\mathrm{col}(\bar{w}_1,\bar{w}_2,\ldots,\bar{w}_N)$. Noting the fact that $\hat{a}_i-a_l^0=0$ for $t\geq T_{11}$, $\forall i\in\mathcal{V}$, $l\in\{1,2,\ldots,J\}$. Then, substituting (30) and (31) into (11) yields that

$$\begin{cases}\dot{\bar{\eta}}=\bar{\varphi}(t)\bar{\eta}+\varphi(t)\bar{w},\\ \dot{\bar{w}}=-\varphi(t)(H\otimes I_3)(\alpha_1\bar{\eta}+\alpha_2\bar{w}).\end{cases} \tag{33}$$

Let $S=\alpha_1\bar{\eta}+\alpha_2\bar{w}$. Taking the derivative of S, it follows that

$$\dot{S}=-\alpha_2\varphi(t)(H\otimes I_3)S+\alpha_1\bar{\varphi}(t)\bar{\eta}+\alpha_1\varphi(t)\bar{w}. \tag{34}$$

According to the definition of H, (34) can be written as

$$\begin{aligned}\dot{S}_1 =& -h_{11}\alpha_2\varphi(t)S_1+\alpha_1\bar{\varphi}(t)\bar{\eta}_1+\alpha_1\varphi(t)\bar{w}_1,\\ \dot{S}_2 =& -\alpha_2\varphi(t)h_{21}S_1-\alpha_2\varphi(t)h_{22}S_2\\&+\alpha_1\bar{\varphi}(t)\bar{\eta}_2+\alpha_1\varphi(t)\bar{w}_2,\\ &\vdots\\ \dot{S}_J =& -\alpha_2\varphi(t)\sum_{l=1}^{J-1}h_{Jl}S_l-\alpha_2\varphi(t)h_{JJ}S_J\\&+\alpha_1\bar{\varphi}(t)\bar{\eta}_J+\alpha_1\varphi(t)\bar{w}_J.\end{aligned} \tag{35}$$

Construct the following Lyapunov function candidate

$$V_{2l}=\frac{1}{2}S_l^TP_lS_l, l\in\{1,2,\ldots,J\}, \tag{36}$$

where P_l is the diagonal matrix with respect to h_{ll}, see Lemma 2 for more details.

Step 1: Suppose $l=1$. It follows that

$$V_{21}=\frac{1}{2}S_1^TP_1S_1. \tag{37}$$

For $t\in[T_{11},T_{11}+T_u)$, taking the derivative of V_{21}, it can be obtained that

$$\begin{aligned}\dot{V}_{21}&=S_1^TP_1(-h_{11}\alpha_2\varphi(t)S_1+\alpha_1\bar{\varphi}(t)\bar{\eta}_1+\alpha_1\varphi(t)\bar{w}_1)\\&=-\frac{1}{2}\alpha_2\varphi(t)S_1^TQ_1S_1+\bar{\varphi}(t)S_1^TP_1(S_1-\bar{w}_1)\\&\quad+\alpha_1\varphi(t)S_1^TP_1\bar{w}_1.\end{aligned} \tag{38}$$

Let $Z_1(t)=\dot{V}_{21}+(b+c\varphi(t))V_{21}$. It then can be derived that

$$\begin{aligned}Z_1(t)=&-\frac{1}{2}\alpha_2\varphi(t)S_1^TQ_1S_1+\bar{\varphi}(t)S_1^TP_1(S_1-\bar{w}_1)\\&+\alpha_1\varphi(t)S_1^TP_1\bar{w}_1+\frac{1}{2}(b+c\varphi(t))S_1^TP_1S_1.\end{aligned} \tag{39}$$

By introducing Lemma 2 and Lemma 4, it can be concluded that

$$\begin{aligned}&\lambda_{\min}(Q_1){S_1}^TS_1\leq{S_1}^T\left(Q_1\otimes I_3\right)S_1\leq\lambda_{\max}(Q_1){S_1}^TS_1,\\ &{S_1}^T\left(P_1\otimes I_3\right)\bar{w}_1=\sum_{i=1}^{n}\zeta_iS_{1i}^T\bar{w}_{1i}\\&\leq\sum_{i=1}^{n}\zeta_i\left(\hbar\|S_{1i}\|^2+\frac{1}{4\hbar}\|\bar{w}_{1i}\|^2\right)\\&\leq\lambda_{\max}(P_1)\left(\hbar{S_1}^TS_1+\frac{1}{4\hbar}\bar{w}_1^T\bar{w}_1\right).\end{aligned} \tag{40}$$

Submitting (40) into (39) yields that

$$Z_1(t)\leq\frac{1}{2}\varphi(t)\lambda_{\max}(P_1)\left[\frac{2}{\rho}+\alpha_1-\frac{\alpha_2}{\rho}+\frac{b}{\varphi(t)}+2c\right]S_1^TS_1$$

$$-\frac{1}{2}\varphi(t)\alpha_2\lambda_{\max}(Q_1)S_1^T S_1 + \frac{1}{2}\varphi(t)\lambda_{\max}(P_1)\left(\alpha_1-\frac{\alpha_2}{\rho}\right)\bar{w}_1^T\bar{w}_1. \quad (41)$$

If (16) holds, it implies that $Z_1(t)\le 0$. It further can be derived that $\dot{V}_{21}\le -(b+c\varphi(t))V_{21}$. Then, based on lemma 1, the following inequality holds

$$V_{21}\le -\mu^{-c}(t)\exp^{-b(t-t_0)}V_{21}(t_0). \quad (42)$$

It can be thus obtained from (1) and (42) that

$$\|\bar{\eta}_1\|^2+\|\bar{w}_1\|^2\le \Gamma_1{}^{-1}\mu^{-c}(t)\exp^{-b(t-t_0)}V_{21}(t_0), \quad (43)$$

where $\Gamma_1=\frac{1}{2}\lambda_{\max}(P_1)\min\{\alpha_1^2,\alpha_2^2\}$. Based on (30), it follows that

$$\|\bar{\eta}_1\|^2+\|\bar{w}_1\|^2=\varphi^2(t)\|\tilde{\eta}_1\|^2+\|\tilde{w}_1\|^2 \ge \Gamma_2\left(\|\tilde{\eta}_1\|^2+\|\tilde{w}_1\|^2\right), \quad (44)$$

where $\Gamma_2=\min\{\rho^2/{T_u}^2,1\}$. Combining (43) with (44), it can then be obtained that

$$\|\tilde{\eta}_1\|^2+\|\tilde{w}_1\|^2\le \frac{1}{\Gamma_1\Gamma_2}\mu^{-c}(t)\exp^{-b(t-t_0)}V_{21}(t_0). \quad (45)$$

Based on Lemma 1, it concludes that $\lim_{t\to T_{11}+T_u}\mu^{-c}(t)=0$. Then, it follows that $\lim_{t\to T_{11}+T_u}\|\tilde{\eta}_1\|=\mathbf{0}$ and $\lim_{t\to T_{11}+T_u}\|\tilde{w}_1\|=\mathbf{0}$. Similar to (38)-(46), for $t\ge T_{11}+T_u$, if (16) holds, we can easily obtain that

$$\begin{aligned}\dot{V}_{21}&\le -bV_{21}-c\varphi(t)V_{21},\\ &=-(b+c\rho/T_u)V_{21},\\ &\le 0.\end{aligned} \quad (46)$$

Hence, it yields that $V_{21}=0$ for $t\ge T_{11}+T_u$, $i\in\mathcal{V}_1$.

Step 2: Suppose $l=2$. According to the analyse above, when $t\ge T_{11}+T_u$, $\dot{S}_2$ can be rewritten as

$$\dot{S}_2=-\alpha_2\varphi(t)h_{22}S_2+\alpha_1\bar{\varphi}(t)\bar{\eta}_2+\alpha_1\varphi(t)\bar{w}_2. \quad (47)$$

Similar to the steps (37)-(46), it can be derived that $\tilde{\eta}_i,\tilde{w}_i$ converge to zero as $t\to T_{11}+2T_u$.

Step 3: For $l=J$, when $t\ge T_{11}+\sum_{l=1}^{J-1}T_u$, it can be concluded that

$$\dot{S}_J=-\alpha_2\varphi(t)h_{JJ}S_J+\alpha_1\bar{\varphi}(t)\bar{\eta}_J+\alpha_1\varphi(t)\bar{w}_J. \quad (48)$$

Based on the mathematical induction, it obtains that $\hat{\eta}_i,\hat{w}_i$ will approach to zero within prescribed time $T_{11}+\sum_{l=1}^{J}T_u$. i.e., $t_0+\sum_{l=1}^{2J}T_u,\forall i\in\mathcal{V},l\in\{1,2,\ldots,J\}$.

Above all, the prescribed-time convergence of $\hat{\eta}_i,\hat{w}_i$ and $\hat{a}_i$ can be achieved in $T_1=t_o+\sum_{l=1}^{2J}T_u$, Namely, for $t>T_1$, it obtains that $\lim_{t\to T_1}\|\hat{\eta}_i-\eta_l^0\|=0$, $\lim_{t\to T_1}\|\hat{w}_i-w_l^0\|=0$, $\lim_{t\to T_1}\|\hat{a}_i-a_l^0\|=0,\forall i\in\mathcal{V},l\in\{1,2,\ldots,J\}$. This ends the proof. ■

C. Analysis of the Fast Fixed-Time Tracking Algorithm

Theorem 2: Suppose that Assumptions 1-4 hold. By using (11) and (13), the fast fixed-time output multi-formation tracking problem of the networked ASVs can be solved and the fast fixed time can be set as $T=T_1+T_u+T_\kappa,\forall i\in\mathcal{V},l\in\{1,2,\ldots,J\}$ if the following conditions hold:

$$\begin{aligned}&2+\alpha_1\rho-\alpha_2+bT_u+c\rho-\alpha_2\rho\frac{\lambda_{\max}(Q_l)}{\lambda_{\max}(P_l)}\le 0,\\ &\rho\alpha_1-\alpha_2\le 0,\\ &\lambda_{\min}(\Pi_i)\ge d_m,\\ &\alpha_3\ge\frac{\lambda_{\max}(P_l)}{\lambda_{\min}(Q_l)},\\ &\beta_3\ge d_a.\end{aligned} \quad (49)$$

Proof: This part aims to prove the fast fixed-time convergence of the tracking errors defined in (12). For $t\ge T_1$, the tracking error (12) equals to the following equation

$$e_i=\eta_i-\eta_l^0-o_i,\quad \dot{e}_i=\dot{\eta}_i-w_l^0. \quad (50)$$

The Lyapunov function is chosen as

$$V_3=\frac{1}{2}s_i^T s_i. \quad (51)$$

Taking the derivative of V_3 obtains that

$$\begin{aligned}\dot{V}_3&=s_i^T\left[\tilde{K}(e_i)\dot{e}_i+K_i(e_i)\dot{e}_i+\gamma_2|\dot{e}_i|^{\gamma_2-1}A_i(\eta_i)\tau_i\right]\\ &\quad+s_i^T\gamma_2|\dot{e}_i|^{\gamma_2-1}(Y_i(\eta_i,v_i)+\bar{d}_i(t)-a_l^0)\\ &\le -\|s_i\|_1\gamma_2|\dot{e}_i|^{\gamma_2-1}(\lambda_{\max}(\Pi)-d_m)\\ &\quad-\delta_\xi\left(|\dot{e}_i|^{\gamma_2-1}\right)(\gamma_3+\gamma_4\varphi(t))V_2.\end{aligned} \quad (52)$$

Then, it follows from $\lambda_{\max}(\Pi)\ge d_m$ that

$$\dot{V}_3\le -\delta_\xi\left(|\dot{e}_i|^{\gamma_2-1}\right)(\gamma_3+\gamma_4\varphi(t))V_3. \quad (53)$$

Then similar to the analysis in [39], it derives that the system (9) will be driven on $s_i=0$ in settling time $t_0+T_u+T_\iota$, in which $T_\iota=(\xi^{1/(\gamma_2-1)})/(\lambda_{\min}(\Pi_i)-d_m)$. Noting that ξ is a sufficiently small parameter, coupled with the limited condition $1<\gamma_2\le 2$ (further illustrates that $0<\xi^{1/(\gamma_2-1)}<<1$), it obtains T_ι is infinitesimal and thus can be omitted here. This leads to the inescapable conclusion that the system (9) will be driven on $s_i=0$ in settling time t_0+T_u. Moreover, once $s_i=0$, $e_i,\dot{e}_i$ converge to zero less than T_κ. Further, it gets that system states achieve fast fixed-time stability within $T=T_1+T_u+T_\kappa$. When $t>T$, the position tracking error of the networked ASVs is

$$\begin{aligned}&\lim_{t\to T}\left\|\eta_i-\eta_l^0-o_i\right\|\\ &=\lim_{t\to T}\left\|\eta_i-\tilde{\eta}_i+\tilde{\eta}_i-\eta_l^0-o_i\right\|\\ &\le\lim_{t\to T}\|\eta_i-\tilde{\eta}_i-o_i\|+\lim_{t\to T}\left\|\tilde{\eta}_i-\eta_l^0\right\|\\ &=\lim_{t\to T}\|e_i\|+\lim_{t\to T}\|\bar{\eta}_i\|\\ &=0.\end{aligned} \quad (54)$$

It further obtains that $\lim_{t\to T}\|w_i-w_l^0\|=0$, $\forall i\in\mathcal{V}$, $l\in\{1,2,\ldots,J\}$. This ends the proof. ■

Remark 3: To make it more clear, the framework of (11) and (13) is provided in Fig. 2 to illustrate the information flow of the

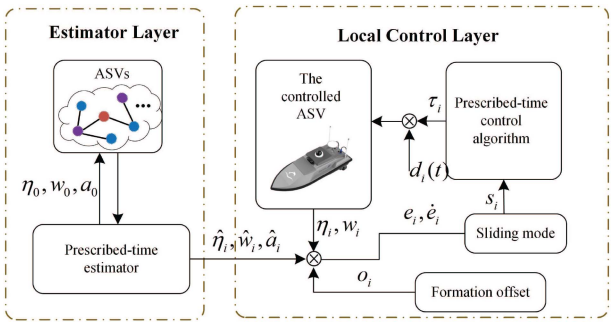

Fig. 2. General framework of the proposed control algorithm.

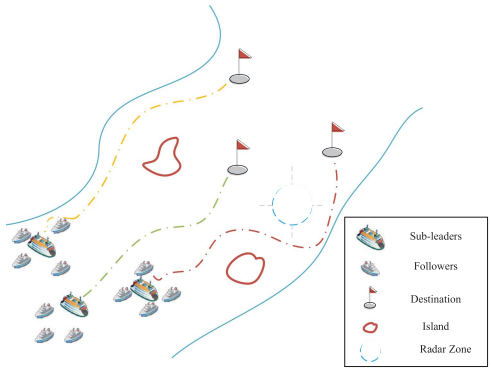

Fig. 3. The ocean exploration scene of the networked ASVs.

Algorithm 1: Design Guidelines of the Algorithm.

Step 1: Set the interaction graph and obtain the gain $\lambda_{max}(Q_l), \lambda_{min}(P_l)$;
Step 2: Set the prescribed time T_u and the related appropriate gain t_0, ρ, b, c according to lemma 1;
Step 3: Set an appropriate gain α_1/α_2 according to the first and second inequalities in conditions (49), and then set the appropriate gains α_1, α_2 respectively;
Step 4: Set the gains α_3, according to the known $\lambda_{max}(Q_l), \lambda_{min}(P_l)$, and set the gains Π, β_3 to satisfy the conditions in (49).

states. It shows that the fast fixed-time control algorithm includes distributed prescribed-time estimator layer and local control layer. The states of the leader is estimated in the prescribed time T_1 in the distributed estimator layer. Then, there are two involved user-designed time in the local control layer, one is that the states of the closed-loop system reach to the sliding surface s_i in the prescribed time $t_0 + T_u$ (where $t_0 = T_1$ holds), the another is that the error states converge to the origin in the fixed time T_κ. Apparently, the whole convergence time is bounded with $T = T_1 + T_u + T_\kappa$. Furthermore, the Algorithm 1 is introduced to illustrate the design procedure of the proposed controller.

Remark 4: Compared with the existing researches of the formation control for the networked ASVs, the designed algorithm in this paper shows several advantages in the following aspects.

1) The multi-formation tracking control shows more efficient in practical application, in which every subnetwork can be employed to implement the respective control operations.
2) The multi-formation tracking can be achieved in a fast fixed time, in which the settling time is independent of the initial conditions.
3) The fast fixed-time stability analysis of the multi-formation tracking has certain difficulties in technical implementation, since the analysis methods of the single-formation tracking problem can not be directly applied to the multi-formation one.

Remark 5: The term $\varphi(t)$ in (1) is essential for realizing the prescribed-time stability of the controlled system. The prescribed-time controller (11) includes both the $\varphi(t)$ and $\varphi^2(t)$. This will inevitably place strain on the analysis of the prescribed-time stability when employing the Lyapunov function. Referring to [31], a state transformation (30) is applied to analyze the effectiveness of (11). Correspondingly, (32) can be obtained according to the specific form of $\varphi(t)$ and (30).

Remark 6: The uncertainties regarding model and external have no impact on the recursive feasibility, since we design the hierarchical fast fixed-time tracking algorithm, where the stability of the distributed prescribed-time estimator and the local control layer is analyzed, respectively. Besides, the uncertainties we considered only exist in the local control layer, where the sliding mode control method is introduced to eliminate the influence of the uncertainties as long as Assumption 4 holds. In addition, the uncertainty of the model parameters are not considered in this paper. However, based on the existing work [48], an extend state observer is employed to reduce the negative effect of the unknown model parameters. Please refer to the model-free approach in [48] for more details.

IV. Simulation Results

To link some practical operation, consider that there is a detection scenario that the networked ASVs are divided into several groups to arrive at the corresponding desired areas respectively. In Fig. 3, there are 3 groups including 11 follower vehicles and 3 sub-leaders. The sub-leaders can be virtual or physical, which play a role in providing a trajectory for the follower vehicles of the related group. Spontaneously, the follower vehicles track their corresponding trajectory of the sub-leaders to accomplish appointed task, such as maritime rescuemilitary detection and underwater surveillance. As for the following simulation for illustrating the validity of the designed algorithm, the model parameters of ASV are selected as the same the well-known CyberShip II in [49].

Example 1: (Fast fixed-time multi-formation tracking) The interaction graph and the corresponding weights of networked ASVs are shown in Fig. 4, in which $\mathcal{V}_1 = \{1, 2, 3\}$, $\mathcal{V}_2 = \{4, 5, 6, 7\}$, $\mathcal{V}_3 = \{8, 9, 10, 11\}$, and the nodes L_1, L_2, L_3 are the leaders of each subgroup. The pinning matrix is $\mathcal{B} = \text{diag}(1, 0, 0, 4, 0, 0, 3, 0, 0, 6, 0)$. Let $\rho = 5, t_0 = 0.01, T_u = 0.5, c = 1, b = 0$, then it get $\alpha_1 = 80, \alpha_2 = 60, \alpha_3 = 50$, $\beta_1 = 7; \beta_2 = 8; \beta_3 = 10$. Let $\Pi_i = 55 I_{2\times 6}$, $T_\kappa = 3.1\ s$, $k_1 = k_2 = 1, k = 1.2, \gamma = 0.5, \gamma_1 = 1.5, \gamma_2 = 2$. The theoretical convergence time is $T = 6.51\ s$. The

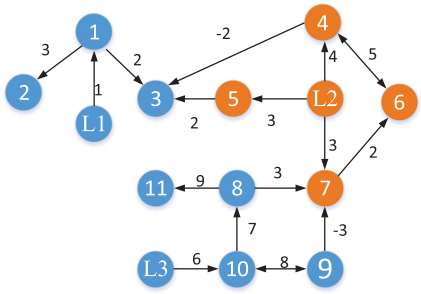

Fig. 4. The interaction graph of the networked ASVs includes 3 subgroups, where $V_1 = \{1, 2, 3\}$, $V_2 = \{4, 5, 6, 7\}$, $V_3 = \{8, 9, 10, 11\}$.

initial values of $\eta_i, w_i, \hat{\eta}_i, \hat{w}_i$ are selected from $[-1, 1]$ randomly. The disturbances are given as $d_i(t) = [0.4\sin(0.02t), 0.4\cos(0.02t), 0.2\cos(0.02t)]^T$. Besides, the formation offsets in the earth-fixed frame are presented as $o_1 = [0, 0.7\sqrt{3}, 0]^T$, $o_2 = [-0.7, 0, 0]^T$, $o_3 = [0.7, 0, 0]^T$, $o_4 = [-0.7, 0.7, 0]^T$, $o_5 = [0.7, 0.7, 0]^T$, $o_6 = [0.7, -0.7, 0]^T$, $o_7 = [-0.7, -0.7, 0]^T$, $o_8 = [0, 0.7, 0]^T$, $o_9 = [0.7, 0, 0]^T$, $o_{10} = [0, -0.7, 0]^T$, $o_{11} = [-0.7, 0, 0]^T$. The desired trajectories of the corresponding leaders are given as

$$\begin{cases} \eta_1^0 = [4\sin(0.5t), 2.5(1-\cos(0.5t), 0.5t]^T, \\ w_1^0 = [2\cos(0.5t), 1.25\sin(0.5t), 0.5]^T, \\ a_1^0 = [-\sin(0.5t), 0.625\cos(0.5t), 0]^T, \end{cases}$$

$$\begin{cases} \eta_2^0 = [5 + 8\sin(0.02t), 2 - 8\cos(0.02t), 0.02t]^T, \\ w_2^0 = [0.16\cos(0.02t), 0.16\sin(0.02t), 0.02]^T, \\ a_2^0 = [-0.0032\sin(0.02t), 0.0032\cos(0.02t), 0]^T, \end{cases}$$

$$\begin{cases} \eta_3^0 = [-0.5 + 2.5\sin(t), 6 - 5\cos(t), t]^T, \\ w_3^0 = [2.5\cos(t), 5\sin(t), 1]^T, \\ a_3^0 = [-2.5\sin(t), 5\cos(t), 0]^T. \end{cases}$$

Based on the above determined control gains, the simulation results are shown in Figs. 5–10. Figs. 5–6 show the convergence process of the estimated states of the networked ASVs, from which $\hat{\eta}_i$, $\hat{w}_i$ and $\hat{a}_i$ estimate the leaders' states η_l^0, w_l^0 and a_l^0 in the prescribed time successfully under (11). Fig. 7 intuitively demonstrates that the control objective in Definition 3 is achieved successfully, of which the estimation $\hat{\eta}_i$, $\hat{w}_i$ and $\hat{a}_i$ can be estimated in the prescribed time and then the tracking errors approach origin in the fast fixed time 6.51 s. Besides, the settling time is independent of the initial conditions. Figs. 8–10 show the formation tracking trajectories of the subnetworks respectively. The outputs of the networked ASVs have formed the predesigned formation pattern successfully in our predesigned settling time.

Example 2: (The illustration of the irrelevant to the initial conditions) Two comparative examples are proposed to show that the convergence time of the fast fixed-time control algorithm is unrelated to the initial conditions, in which the initial values

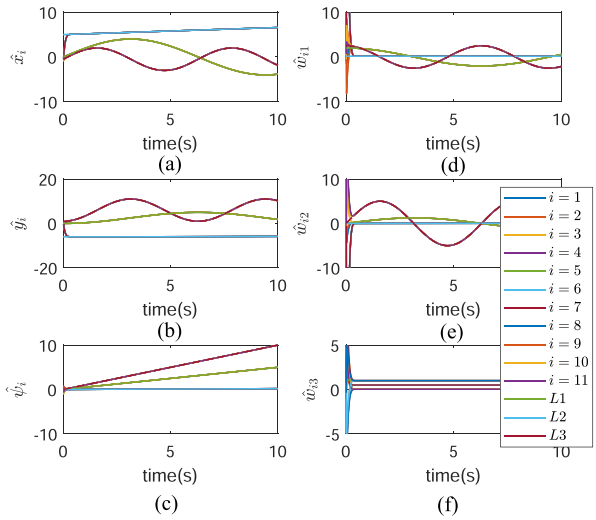

Fig. 5. Pictures (a)-(c) is the evolution of the estimated position $\hat{\eta}_i$; pictures (d)-(f) is the evolution of the estimated velocity $\hat{w}_i$.

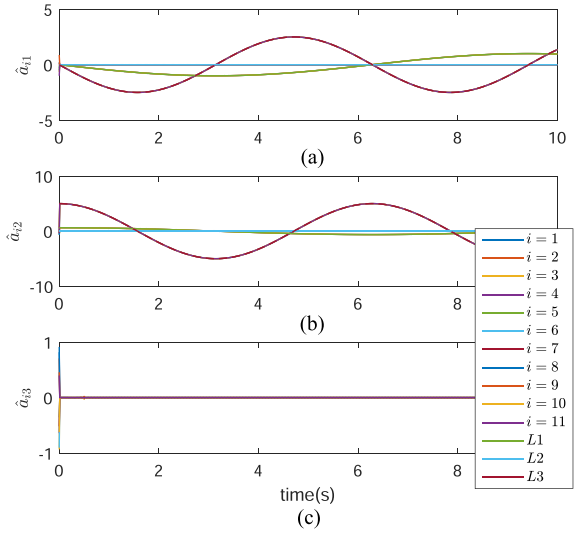

Fig. 6. The evolution of the estimated acceleration $\hat{a}_i$.

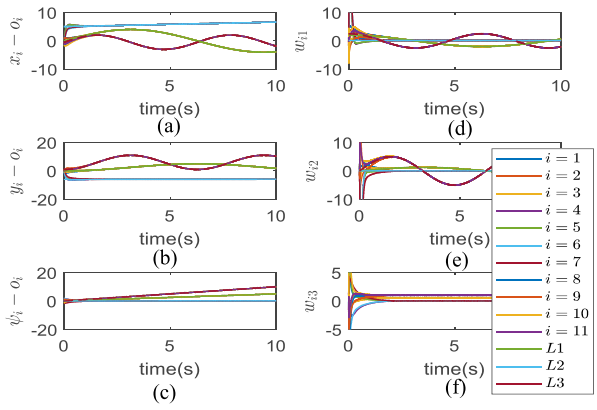

Fig. 7. Pictures (a)-(c) is the evolution of the position η_i in earth-fixed frame. Pictures (d)-(f) is the evolution of the velocity w_i in earth-fixed frame.

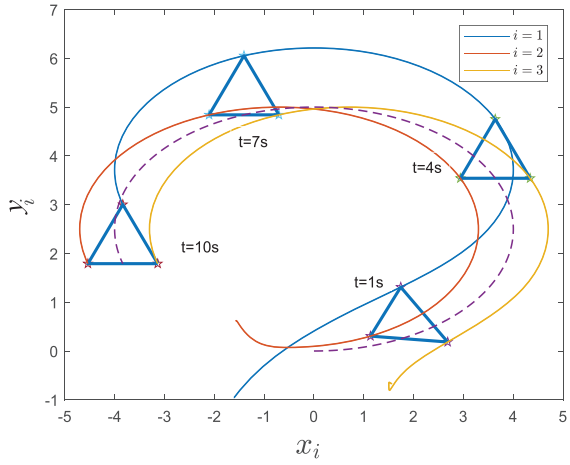

Fig. 8. The formation tracking trajectories of the first subnetwork.

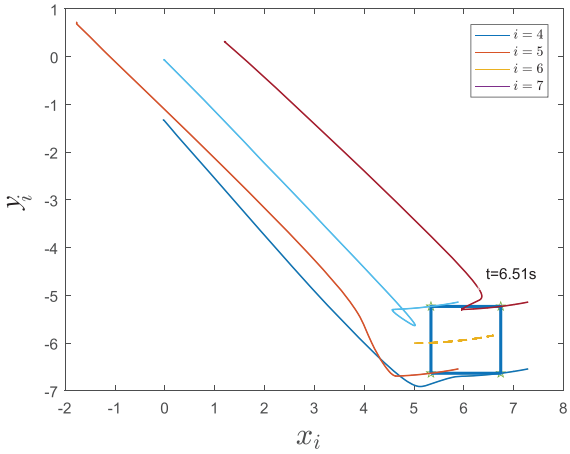

Fig. 9. The formation tracking trajectories of the second subnetwork.

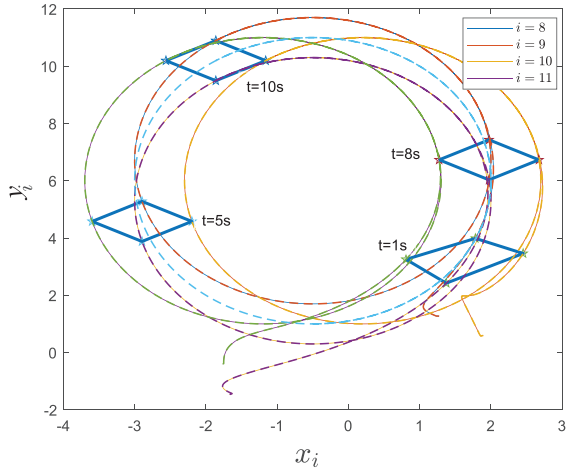

Fig. 10. The formation tracking trajectories of the third subnetwork.

are selected at the interval of $[-1, 1]$ and $[-1000, 1000]$, respectively. The control parameters are chosen as the same as Example 1. By comparison, from the tracking errors demonstrated in Figs. 11 and 12, it can be derived that both the position tracking error e_i and the velocity tracking error $\dot{e}_i$ in the earth-fixed frame

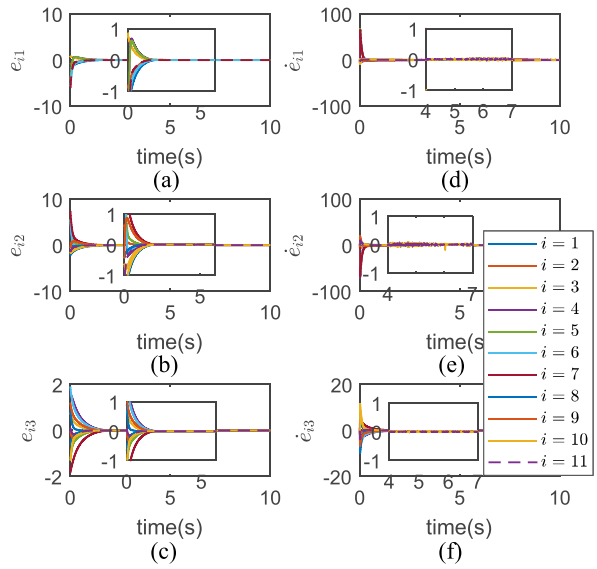

Fig. 11. The evolution of the tracking errors with the initial conditions ranged from [-1,1].

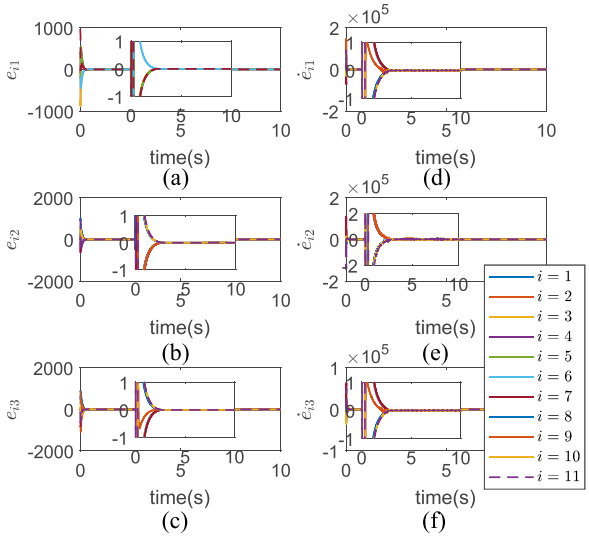

Fig. 12. The evolution of the tracking errors with the initial conditions ranged from [-1000,1000].

converge to the origin in T, even though the initial values vary enormously under the two simulations. Further, it can safely come to the conclusion that the fast fixed time T is independent of the initial conditions.

Example 3: (The comparison with the fixed-time and finite-time control law) Based on the discussion in Remark 2, several comparisons with the existing fixed-time and finite-time control algorithms are carried out to show the fast convergence rate of the proposed algorithm. To this end, the initial conditions and the time-varying targets, as well as the interaction topology are chosen the same (i.e., the second network in Fig. 4). Firstly, the finite-time algorithm in [20] is employed to replace the estimator

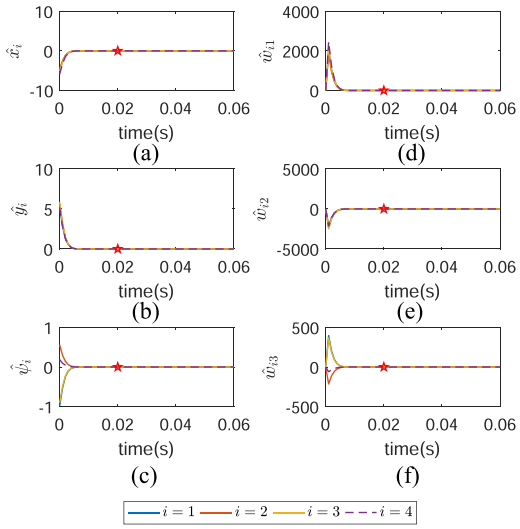

Fig. 13. The evolution of the tracking errors using the designed fast fixed-time estimator algorithm.

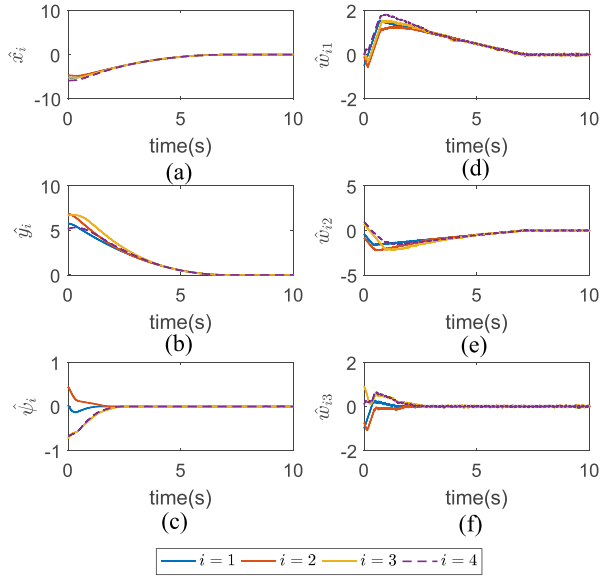

Fig. 14. The evolution of the tracking errors using the finite-time control algorithm.

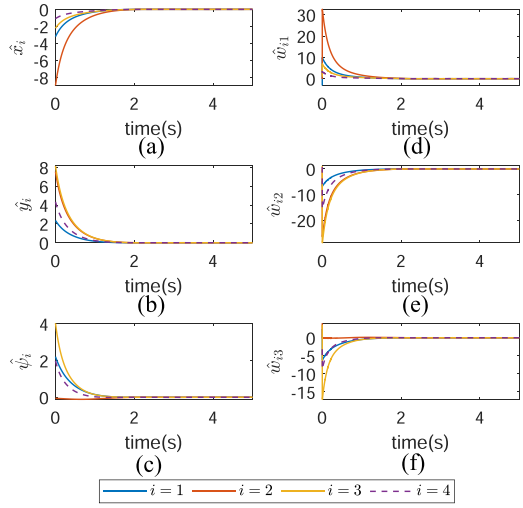

Fig. 15. The evolution of the tracking errors using the fixed-time control algorithm.

layer (11) and is presented as

$$\begin{cases} \dot{\hat{\eta}}_i = \hat{w}_i, \\ \dot{\hat{w}}_i = -\xi_1 \mathrm{sgn}\Big\{\xi_2 \mathrm{sig}[b_i(\hat{\eta}_i - \eta_l^0) + \sum_{j\in\mathcal{N}_i} a_{ij}(\hat{\eta}_i - \hat{\eta}_j)]^{\frac{1}{2}} \\ \qquad + b_i(\hat{w}_i - w_l^0) + \sum_{j\in\mathcal{N}_i} a_{ij}(\hat{w}_i - \hat{w}_j)\Big\}. \end{cases} \tag{55}$$

Although the settling time of (55) are set as small as possible by adjusting the control parameters and initial conditions, it still needs lager convergence time than the controller we designed. Secondly, we compared the fixed-time controller in [39], where the fixed-time sliding mode control method are utilized in the controller design and the reaching time to the sliding surface are associated with the several control parameters. Refer to [39] for more details about the convergence time and the form of the fixed-time algorithm is given as follows.

$$\begin{cases} \dot{\hat{\eta}}_i = \hat{w}_i, \\ \dot{\hat{w}}_i = \Big(\sum_{j=1}^N a_{ij} + b_i\Big)^{-1} \\ \qquad \Big\{\sum_{j=1}^N a_{ij}\dot{\hat{w}}_j - \frac{1}{\gamma_2}\Big(\tilde{K}(\theta_{i1}) + K(\theta_{i1})\Big) \\ \qquad \times \mathrm{sig}^{2-\gamma_2}(\theta_{i2}) - \frac{1}{\gamma_2}\mathrm{diag}\{\mu_\tau(|\theta_{i2}|^{\gamma_2-1})\Big\} \\ \qquad \times \mathrm{diag}\{|\theta_{i2}|^{1-\gamma_2}\}\mathrm{sig}^{\gamma_5}(\tau_i \mathrm{sig}^{\gamma_3}(S_i) + \delta_i)\mathrm{sig}^{\gamma_4}(S_i)\}. \end{cases} \tag{56}$$

The specific conditions of the control parameters can be found in [39] and is omitted for space limitation.

The simulation results can be observed in Figs. 13–15. It demonstrates that the designed algorithm can achieve fast convergence performance than the general finite-time and fixed-time control laws. Specifically, it can be observed from Fig. 13 that the settling time of the designed algorithm is set at 0.02 s. This displays the superiority of the designed algorithm for realizing the control objective within any arbitrarily convergence time. Besides, Fig. 14 shows the evolution of the tracking errors under the finite-time control and the settling time can not be set as small as the designed algorithm. From Fig. 15, the settling time of the general fixed-time control is also longer than the designed algorithm, although the fixed-time sliding surface in (56) is the same as that in (13). This is because the reaching time to the sliding surface of (56) is related to several control parameters, which can be further seen in [39]. However, the reaching time to the sliding surface of (13) can be set artificially and arbitrarily, even to 0.02 s. Above all, the faster convergence rate could be guaranteed under the designed fast fixed-time control algorithm.

V. Conclusion

In this paper, a novel fast fixed-time tracking control algorithm has been proposed to solve output multi-formation tracking problem of the networked ASVs with external disturbances

under directed graph. The proposed algorithm is capable of guaranteeing satisfactory tracking performances in a fast fixed-time manner. Accordingly, an appropriate mathematical induction-based method has been introduced into stability analysis for dealing with the multi-formation tracking problem. The sufficient conditions for achieving fast fixed-time multi-formation tracking of the networked ASVs have been obtained by employing the mathematical induction method and the Lyapunov stability theory. Finally, several illustrative simulation examples have been presented to demonstrate the superiorities of the fast fixed-time control algorithm. Future work will be focused on the prescribed-time multi-formation tracking control of the networked ASVs with input constraint.

REFERENCES

[1] J. Zhang, J. Yan, and P. Zhang, "Multi-UAV formation control based on a novel back-stepping approach," *IEEE Trans. Veh. Technol.*, vol. 69, no. 3, pp. 2437–2448, Mar. 2020.

[2] G. Zhu, Y. Ma, Z. Li, R. Malekian, and M. Sotelo, "Event-triggered adaptive neural fault-tolerant control of underactuated MSVs with input saturation," *IEEE Trans. Intell. Transp. Syst.*, vol. 23, no. 7, pp. 7045–7057, Jul. 2022.

[3] L. Liu, D. Wang, Z. Peng, T. Li, and C. L. P. Chen, "Cooperative path following ring-networked under-actuated autonomous surface vehicles: Algorithms and experimental results," *IEEE Trans. Cybern.*, vol. 50, no. 4, pp. 1519–1529, Apr. 2020.

[4] Z. Peng, J. Wang, D. Wang, and Q.-L. Han, "An overview of recent advances in coordinated control of multiple autonomous surface vehicles," *IEEE Trans. Ind. Informat.*, vol. 17, no. 2, pp. 732–745, Feb. 2021.

[5] N. Gu, D. Wang, Z. Peng, and L. Liu, "Distributed containment maneuvering of uncertain under-actuated unmanned surface vehicles guided by multiple virtual leaders with a formation," *Ocean Eng.*, vol. 187, 2019, Art. no. 105996.

[6] J. Yu, W. Xiao, X. Dong, Q. Li, and Z. Ren, "Practical formation-containment tracking for multiple autonomous surface vessels system," *IET Control Theory Appl.*, vol. 13, no. 17, pp. 2894–2905, 2019.

[7] W. Zhou, Y. Wang, C. K. Ahn, J. Cheng, and C. Chen, "Adaptive fuzzy backstepping-based formation control of unmanned surface vehicles with unknown model nonlinearity and actuator saturation," *IEEE Trans. Veh. Technol.*, vol. 69, no. 12, pp. 14749–14764, Dec. 2020.

[8] S. He, M. Wang, S.-L. Dai, and F. Luo, "Leader-follower formation control of USVs with prescribed performance and collision avoidance," *IEEE Trans. Ind. Informat.*, vol. 15, no. 1, pp. 572–581, Jan. 2019.

[9] G. Zhu, Y. Ma, Z. Li, R. Malekian, and M. Sotelo, "Adaptive neural output feedback control for MSVs with predefined performance," *IEEE Trans. Veh. Technol.*, vol. 70, no. 4, pp. 2994–3006, Apr. 2021.

[10] M. Van, "An enhanced tracking control of marine surface vessels based on adaptive integral sliding mode control and disturbance observer," *ISA Trans.*, vol. 90, pp. 30–40, 2019.

[11] J. X. Zhang and G. H. Yang, "Fault-tolerant fixed-time trajectory tracking control of autonomous surface vessels with specified accuracy," *IEEE Trans. Ind. Electron.*, vol. 67, no. 6, pp. 4889–4899, Jun. 2020..

[12] Z. Zheng, "Moving path following control for a surface vessel with error constraint," *Automatica*, vol. 118, 2020, Art. no. 109040.

[13] D. Belleter, M. A. Maghenem, C. Paliotta, and K. Y. Pettersen, "Observer based path following for underactuated marine vessels in the presence of ocean currents: A global approach," *Automatica*, vol. 100, pp. 123–134, 2019.

[14] S. Song, J. H. Park, B. Zhang, and X. Song, "Event-triggered adaptive practical fixed-time trajectory tracking control for unmanned surface vehicle," *IEEE Trans. Circuits Syst. II: Exp. Briefs*, vol. 68, no. 1, pp. 436–440, Jan. 2021.

[15] J. Ghommam and M. Saad, "Adaptive leader-follower formation control of underactuated surface vessels under asymmetric range and bearing constraints," *IEEE Trans. Veh. Technol.*, vol. 67, no. 2, pp. 852–865, Feb. 2018.

[16] Y. Lu, R. Su, C. Zhang, and L. Qiao, "Event-triggered adaptive formation keeping and interception scheme for autonomous surface vehicles under malicious attacks," *IEEE Trans. Ind. Informat.*, vol. 18, no. 6, pp. 3947–3957, Jun. 2022.

[17] J. Li, J. Du, and W. J. Chang, "Robust time-varying formation control for underactuated autonomous underwater vehicles with disturbances under input saturation," *Ocean Eng.*, vol. 179, pp. 180–188, 2019.

[18] L. Qiao and W. Zhang, "Trajectory tracking control of AUVs via adaptive fast nonsingular integral terminal sliding mode control," *IEEE Trans. Ind. Informat.*, vol. 16, no. 2, pp. 1248–1258, Feb. 2020.

[19] T. Han, Z. H. Guan, M. Chi, B. Hu, T. Li, and X. H. Zhang, "Multi-formation control of nonlinear leader-following multi-agent systems," *ISA Trans.*, vol. 69, pp. 140–147, 2017.

[20] C.-D. Liang, M.-F. Ge, Z.-W. Liu, Y.-W. Wang, and H. R. Karimi, "Output multiformation tracking of networked heterogeneous robotic systems via finite-time hierarchical control," *IEEE Trans. Cybern.*, vol. 51, no. 6, pp. 2893–2904, Jun. 2021.

[21] J. W. Dong, C. D. Liang, M. F. Ge, T. F. Ding, X. W. Zhao, and Z. W. Liu, "Finite-time multi-target tracking of networked Euler-Lagrange systems via hierarchical active disturbance rejection control," *Int. J. Control*, vol. 95, pp. 2743–2757, 2021, doi: 10.1080/00207179.2021.1934548.

[22] X. Dong, Y. Li, C. Lu, G. Hu, Q. Li, and Z. Ren, "Time-varying formation tracking for UAV swarm systems with switching directed topologies," *IEEE Trans. Neural Netw. Learn. Syst.*, vol. 30, no. 12, pp. 3674–3685, Dec. 2019.

[23] J. Hu, B. Lennox, and F. Arvin, "Robust formation control for networked robotic systems using Negative Imaginary dynamics," *Automatica*, vol. 140, 2022, Art. no. 110235.

[24] Y. Tang, D. Zhang, P. Shi, W. Zhang, and F. Qian, "Event-based formation control for nonlinear multiagent systems under DoS attacks," *IEEE Trans. Autom. Control*, vol. 66, no. 1, pp. 452–459, Jan. 2021.

[25] S. Zuo and D. Yue, "Resilient output formation containment of heterogeneous multigroup systems against unbounded attacks," *IEEE Trans. Cybern.*, vol. 52, no. 3, pp. 1902–1910, Mar. 2022.

[26] J. Yu, P. Shi, and L. Zhao, "Finite-time command filtered backstepping control for a class of nonlinear systems," *Automatica*, vol. 92, pp. 173–180, 2018.

[27] C. C. Chen and Z. Y. Sun, "A unified approach to finite-time stabilization of high-order nonlinear systems with an asymmetric output constraint," *Automatica*, vol. 111, 2020, Art. no. 108581.

[28] L. Fang, L. Ma, S. Ding, and J. H. Park, "Finite-time stabilization of high-order stochastic nonlinear systems with asymmetric output constraints," *IEEE Trans. Syst., Man, Cybern. Syst.*, vol. 51, no. 11, pp. 7201–7213, Nov. 2021.

[29] R. Olfati-Saber and R. M. Murray, "Consensus problems in networks of agents with switching topology and time-delays," *IEEE Trans. Autom. Control*, vol. 49, no. 9, pp. 1520–1533, Sep. 2004.

[30] G. Guo and P. Zhang, "Asymptotic stabilization of USVs with actuator dead-zones and yaw constraints based on fixed-time disturbance observer," *IEEE Trans. Veh. Technol.*, vol. 69, no. 1, pp. 302–316, Jan. 2020.

[31] Y. Kim and M. Mesbahi, "On maximizing the second smallest eigenvalue of a state-dependent graph Laplacian," *IEEE Trans. Autom. Control*, vol. 51, no. 1, pp. 116–120, Jan. 2006.

[32] N. Wang and H. Li, "Leader-follower formation control of surface vehicles: A fixed-time control approach," *ISA Trans.*, vol. 124, pp. 356–364, 2022.

[33] Y. Zhao, Y. Zhou, Y. Liu, G. Wen, and P. Huang, "Fixed-time bipartite synchronization with a pre-appointed settling time over directed cooperative cantagonistic networks," *Automatica*, vol. 123, 2021, Art. no. 109301.

[34] Y. Wang, Y. Song, D. J. Hill, and M. Krstic, "Prescribed-time consensus and containment control of networked multiagent systems," *IEEE Trans. Cybern.*, vol. 49, no. 4, pp. 1138–1147, Apr. 2019.

[35] Y. Ren, W. Zhou, Z. Li, L. Liu, and Y. Sun, "Prescribed-time cluster lag consensus control for second-order non-linear leader-following multiagent systems," *ISA Trans.*, vol. 109, pp. 49–60, 2021.

[36] A. J. Munoz-Vazquez, J. D. Sanchez-Torres, E. Jimenez-Rodriguez, and A. G. Loukianov, "Predefined-time robust stabilization of robotic manipulators," *IEEE Trans. Mechatronics*, vol. 24, no. 3, pp. 1033–1040, Jun. 2019.

[37] C. D. Liang, M. F. Ge, Z. W. Liu, G. Ling, and X. W. Zhao, "A novel sliding surface design for predefined-time stabilization of Euler-Lagrange systems," *Nonlinear Dyn.*, vol. 106, no. 1, pp. 445–458, 2021.

[38] H. M. Becerra, C. R. Vazquez, G. Arechavaleta, and J. Delfin, "Predefined-time convergence control for high-order integrator systems using time base generators," *IEEE Trans. Control Syst. Technol.*, vol. 26, no. 5, pp. 1866–1873, Sep. 2018.
[39] Y. Huang and Y. Jia, "Fixed-time consensus tracking control for second-order multi-agent systems with bounded input uncertainties via NFFTSM," *IET Control Theory Appl.*, vol. 11, no. 16, pp. 2900–2909, 2017.
[40] J. Qin and C. Yu, "Cluster consensus control of generic linear multi-agent systems under directed topology with acyclic partition," *Automatica*, vol. 49, no. 9, pp. 2898–2905, 2013.
[41] H. Zhang, Z. Li, Z. Qu, and F. L. Lewis, "On constructing lyapunov functions for multi-agent systems," *Automatica*, vol. 58, pp. 39–42, 2015.
[42] W. He, W. Yu, L. Yao, and G. Chen, "Fully-distributed finite-time consensus of second-order multi-agent systems on a directed network," in *Proc. IEEE Int. Symp. Circuits Syst.*, 2018, pp. 1–4.
[43] Y. Zhou and G. Zhang, "Distributed finite-time lag-consensus for second-order nonlinear multi-agent systems with disturbances," in *Proc. 13th World Congr. Intell. Control Automat.*, 2018, pp. 1594–1599.
[44] T. I. Fossen, *Marine Control Systems: Guidance, Navigation, and Control of Ships, Rigs and Underwater Vehicles*. Trondheim, Norway: Marine Cybernetics, 2002.
[45] J. Zhang, S. Yu, and Y. Yan, "Fixed-time extended state observer-based trajectory tracking and point stabilization control for marine surface vessels with uncertainties and disturbances," *Ocean Eng.*, vol. 186, 2019, Art. no. 106109.
[46] D. Chen, J. Zhang, and Z. Li, "A novel fixed-time trajectory tracking strategy of unmanned surface vessel based on the fractional sliding mode control method," *Electronics*, vol. 11, no. 5, 2022, Art. no. 726.
[47] L. Qiao and W. Zhang, "Adaptive second-order fast nonsingular terminal sliding mode tracking control for fully actuated autonomous underwater vehicles," *IEEE J. Ocean. Eng.*, vol. 44, no. 2, pp. 363–385, Apr. 2019.
[48] K. T. Xu, M. F. Ge, C. D. Liang, T. F. Ding, and X. S. Zhan, "Predefined-time time-varying formation control of networked autonomous surface vehicles: A velocity-and model-free approach," *Nonlinear Dyn.*, vol. 108, pp. 3605–3622, 2022.
[49] C. Yuan, S. Licht, and H. He, "Formation learning control of multiple autonomous underwater vehicles with heterogeneous nonlinear uncertain dynamics," *IEEE Trans. Cybern.*, vol. 48, no. 10, pp. 2920–2934, Oct. 2018.

Teng-Fei Ding (Graduate Student Member, IEEE) received the B.S. degree in mechanical design, manufacturing and automation, the M.S. degree mechanical engineering, and the Ph.D. degree in geological equipment engineering from China University of Geosciences, Wuhan, China, in 2011, 2014, and 2022, respectively. He is currently a Lecturer with the School of Mechanical Engineering and Electronic Information, China University of Geosciences, Wuhan. His research interests include networked robotic systems, distributed control, and reinforcement learning.

Kun-Ting Xu received the B.S. degree from the School of Mechanical Engineering and Electronic Information, China University of Geosciences, Wuhan, China, in 2020. She is currently working toward the M.S. degree with the School of Mechanical Engineering and Electronic Information, China University of Geosciences, Wuhan. Her research interests include networked marine surface vehicles, networked robotic systems, and prescribed-time control.

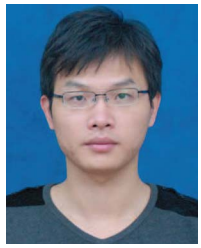

Ming-Feng Ge (Member, IEEE) received the B.Sc. degree in automatic control, and the Ph.D. degree in control theory and control engineering from the Huazhong University of Science and Technology, Wuhan, China, in 2004 and 2016, respectively. He is currently a Professor with the School of Mechanical Engineering and Electronic Information, China University of Geosciences, Wuhan, and he is also with the School of Automation, Central South University, Changsha, China. He has been the Head of the Department of Mechanical Engineering, School of Mechanical Engineering and Electronic Information, China University of Geosciences since 2021. His research interests include networked robotic systems, distributed control, and human-in-the-loop systems.

Ju H. Park (Senior Member, IEEE) received the Ph.D. degree in electronics and electrical engineering from Pohang University of Science and Technology (POSTECH), Pohang, South Korea, in 1997. From May 1997 to February 2000, he was a Research Associate with Engineering Research Center-Automation Research Center, POSTECH. He joined Yeungnam University, Kyongsan, Republic of Korea, in March 2000, where he is currently the Chuma Chair Professor. He is a co-author of the monographs *Recent Advances in Control and Filtering of Dynamic Systems with Constrained Signals (New York, NY, USA: Springer-Nature, 2018)* and *Dynamic Systems With Time Delays: Stability and Control (New York, NY, USA: Springer-Nature, 2019)* and is the Editor of an edited volume *Recent Advances in Control Problems of Dynamical Systems and Networks (New York: Springer-Nature, 2020)*. He has authored or coauthored a number of articles in his research field which include robust control and filtering, neural/complex networks, fuzzy systems, multiagent systems, and chaotic systems. Since 2015, he has been the recipient of the Highly Cited Researchers Award by Clarivate Analytics (formerly, Thomson Reuters) and listed in three fields, Engineering, Computer Sciences, and Mathematics, in 2019–2022. He is also the Editor of the *International Journal of Control, Automation and Systems*. He is also a Subject Editor/Advisory Editor/Associate Editor/Editorial Board Member of several international journals, including *IET Control Theory & Applications, Applied Mathematics and Computation, Journal of The Franklin Institute, Nonlinear Dynamics, Engineering Reports, Cogent Engineering*, the IEEE TRANSACTION ON FUZZY SYSTEMS, the IEEE TRANSACTION ON NEURAL NETWORKS AND LEARNING SYSTEMS, and the IEEE TRANSACTION ON CYBERNETICS. Prof. Park is a Fellow of the Korean Academy of Science and Technology.

Chang-Duo Liang (Graduate Student Member, IEEE) received the B.S. degree from the School of Mechanical Engineering from Wuhan Polytechnic University, Wuhan, China, in 2015. He is currently working toward the Ph.D. degree in geological equipment engineering from the China University of Geosciences, Wuhan. He is also with the College of Mechatronics and Control Engineering, Hubei Normal University, Huangshi, China. His research interests include networked marine surface vehicles, cyber-physical systems and predefined-time sliding mode control.